

# Beneficial Effects of a Blended Fibroin/Aloe Gel Extract Film on the Biomolecular Mechanism(s) *via* the MAPK/ERK Pathway Relating to Diabetic Wound Healing

Preeyawass Phimnuan, Zélie Dirand, Marion Tissot, Saran Worasakwutiphong, Anuphan Sittichokechaiwut, François Grandmottet, Jarupa Viyoch,\* and Céline Viennet\*



Cite This: *ACS Omega* 2023, 8, 6813–6824



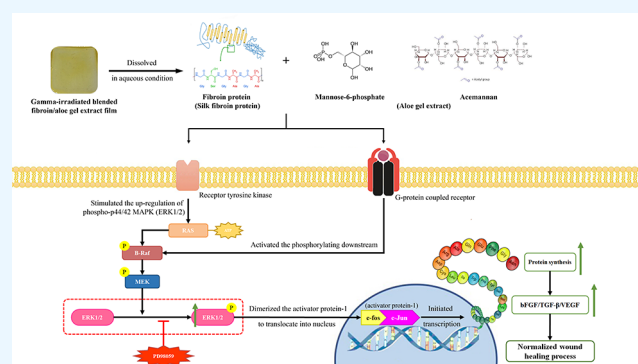
Read Online

ACCESS |

Metrics & More

Article Recommendations

**ABSTRACT:** In diabetic patients, the process of wound healing is usually delayed or impaired. A diabetic environment could be associated with dermal fibroblast dysfunction, reduced angiogenesis, the release of excessive proinflammatory cytokines, and senescence features. Alternative therapeutic treatments using natural products are highly demanded for their high potential of bioactive activity in skin repair. Two natural extracts were combined to develop fibroin/aloe gel wound dressing. Our previous studies revealed that the prepared film enhances the healing rate of diabetic foot ulcers (DFUs). Moreover, we aimed to explore its biological effects and underlying biomolecular mechanisms on normal dermal, diabetic dermal, and diabetic wound fibroblasts. Cell culture experiments showed that the  $\gamma$ -irradiated blended fibroin/aloe gel extract film promotes skin wound healing by enhancing cell proliferation and migration, vascular epidermal growth factor (VEGF) secretion, and cell senescence prevention. Its action was mainly linked to the activation of the mitogen-activated protein kinases/extracellular signal-regulated kinase (MAPK/ERK) signaling pathway known to regulate various cellular activities, including proliferation. Therefore, the findings of this study confirm and support our previous data. The blended fibroin/aloe gel extract film displays a biological behavior with favorable properties for delayed wound healing and can be considered as a promising therapeutic approach in the treatment of diabetic nonhealing ulcers.



## 1. INTRODUCTION

A chronic diabetic foot ulcer (DFU) is described as delayed wound healing leading to amputation in impaired glucose tolerance patients. About 15–25% of diabetic patients are expected to face this complication.<sup>1</sup> The prevention of DFU is complicated regarding the adverse incidences on a patient's well-being, and the prevalence is mainly associated with a number of factors that involves cutaneous cell malfunction and growth factor disorder.<sup>2</sup> Dermal fibroblasts play an important role in skin structure formation and maintenance of homeostasis, including skin barrier construction, extracellular matrix (ECM) production, and angiogenesis support. The decrease of proliferative and mitogenic abilities to the essential growth factors, as well as the deficiency of collagen and enzymatic production, occurs in diabetic ulcer fibroblasts compared to normal fibroblasts.<sup>3</sup> In the molecular pathway, the metabolic abnormalities cause insufficient cellular growth factor responses, including transforming growth factor (TGF- $\beta$ 1), platelet-derived growth factor (PDGF), basic fibroblast growth factor (bFGF), and especially vascular epidermal growth factor (VEGF).<sup>4,5</sup> During normal wound healing, these growth factors

play important roles in the inflammatory and proliferative processes simultaneously with re-epithelialization.<sup>6</sup> They regulate cellular responses and stimulate intracellular signaling pathways involved in the regulation of cell proliferation, differentiation, migration, and protein synthesis. In diabetes conditions, the healing process is dysfunctional by the changes in the levels and timing of TGF- $\beta$ 1, PDGF, bFGF, and VEGF expression.<sup>7</sup> Downregulation of these signals significantly reduces cell migration and proliferation, vasculature remodeling, and maturation, showing critical defects in skin damage repair. Furthermore, deregulated mitogen-activated protein kinase (MAPK) signaling cascades such as extracellular signal-regulated protein kinase (ERK), p38 MAPK (p38), and c-Jun

Received: November 23, 2022

Accepted: January 23, 2023

Published: February 7, 2023



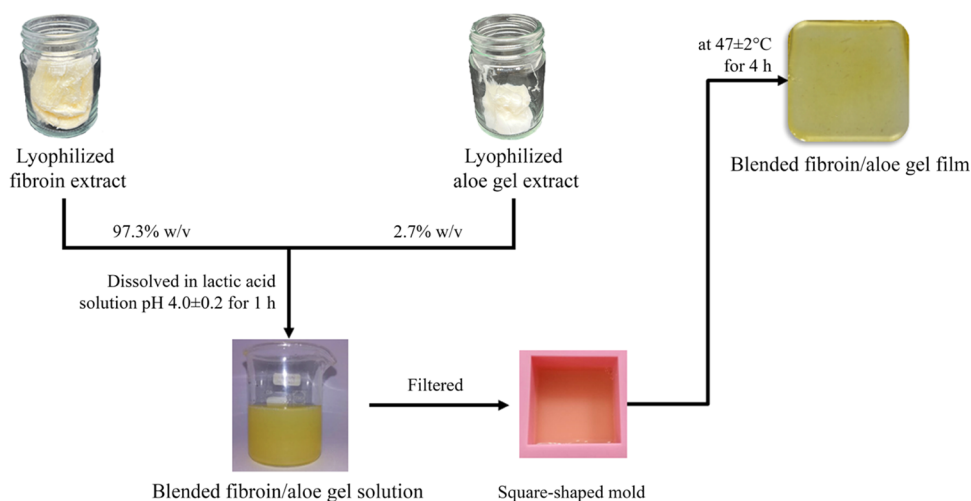


**Figure 1.** Preparation procedure of the blended fibroin/aloë gel extract film.

NH<sub>2</sub>-terminal protein kinase (JNK) have significant effects on wound healing.<sup>8</sup> The overproduction of glucose induces oxidative stress and/or glycation that contribute to impaired activation of growth factor receptors and serine/threonine kinases, resulting in downregulation of ERK1/2 activity.<sup>9,10</sup>

We believe that primary healthcare systems and medical innovations involved in the treatment and management of DFU are essential. Wound dressing is an alternatively practical tool that plays a pivotal role in managing diabetic foot ulcers.<sup>11</sup> Composed of natural products, they have frequently proved their efficacy in the treatment of skin disorders. The cooperation of silk fibroin and aloë gel extract biomaterials has illustrated potential properties in promoting wound healing in *in vitro* and *in vivo* models, as well as in clinical trials.<sup>12,13</sup>

Fibroin protein, comprising the silk cocoon of *Bombyx mori*, illustrates the remarkable biocompatibility to several cells and tissues because of its potent properties in the stimulation of the migration and proliferation of fibroblasts.<sup>12,14</sup> Furthermore, at the molecular level, silk fibroin accelerates signals, including AKT/mTOR and MAPK pathways extensively involved in cell migration and proliferation regulation.<sup>15</sup> Regarding its excellent ability, silk fibroin can be considered as a bioactive material for wound dressing in the medical field.

*Aloe vera* (*Aloe barbadensis* Miller) has been broadly utilized for several traditional therapeutics, especially for wound healing properties. Many productive components consisting of *Aloe vera* exert accelerating effects on fibroblast proliferation and migration in wound granulation tissue.<sup>16</sup> For the cellular pathway, *Aloe vera* stimulates wound repair by promoting collagen type I synthesis, influencing the cyclin-dependent cell cycle progression, stimulating cross-linking of collagen for wound contraction and promoting wound-breaking strength.<sup>17</sup> In addition, *Aloe vera* increases the expression of VEGF and TGF- $\beta$ 1 genes in the wound of diabetes-induced rats.<sup>18</sup> Hence, it clarifies the enhancing capabilities of growth factor expression associated with the wound healing process *via* easy penetration across the skin.<sup>19</sup>

Our previous studies found that the blended fibroin/aloë gel extract film demonstrates potential healing effects, based on experimentations *in vitro* and *in vivo* in streptozotocin-induced diabetic rats, and clinical trials in diabetic foot ulcer patients.<sup>12,13</sup> Additionally, the  $\gamma$ -irradiated developed film enhanced the proliferation and migration of the healthy fibroblast cells. The

presence of functional groups in the blended fibroin/aloë gel film, including amides (I, II, III), glucan units, pyranoside ring, and mannose, promotes tissue repair, but the underlying molecular mechanism is still unclear.<sup>20</sup> In this present study, we explored the beneficial effects of the  $\gamma$ -irradiated blended fibroin/aloë gel extract film on cell biological activities and biomolecular mechanism(s) using normal dermal, diabetic dermal, and diabetic wound fibroblasts. The *in vitro* experiments confirmed that our extract film promotes skin wound healing by enhancing cell viability, proliferation, migration, and VEGF secretion as well as inhibiting cell senescence. The activation of the MAPK signaling pathway, particularly ERK1/2, was involved in the underlying molecular mechanism. We likewise indicate that the developed film is appropriate for managing normal or chronic skin wounds such as DFU.

## 2. MATERIALS AND METHODS

**2.1. Ethical Statement.** The experiment was approved by the medical ethics committee of Besançon University Hospital, France, and patients were informed about the purpose of the research study and provided written consent (protocol 2010-104). We confirm that all methods were performed in accordance with the relevant guidelines and regulations.

**2.2. Materials.** Yellow silkworm cocoons (*Bombyx Mori*, Nang-Laai strain, Chiang Mai Province, Thailand) were received by Queen Sirikit Sericulture Center, Chiang Mai Province, Thailand. *Aloe vera* was cultured and collected from Phitsanulok Province, Thailand. Dulbecco's modified Eagle's medium (DMEM), fetal bovine serum (FBS), penicillin–streptomycin (PS, 10,000 U/mL), 0.05% trypsin/0.02% EDTA, and Dulbecco's phosphate buffer saline (DPBS) were purchased from PAN Biotech, Dominique Dutscher, France. Thiazolyl blue tetrazolium bromide (MTT reagent), lactic acid solution (88%), dimethyl sulfoxide (DMSO), 4',6-diamidino-2'-phenylindole dihydrochloride (DAPI), bovine serum albumin (BSA), propidium iodide (PI), copper(II) sulfate solution, bicinechonic acid solution, protease inhibitor cocktail, Triton X-100, formaldehyde solution 4%, MEK/ERK inhibitor PD98059, phalloidin–tetramethylrhodamine B isothiocyanate, and senescence cells histochemical staining kit were purchased from Sigma-Aldrich Co. Human VEGF ELISA kit was purchased from Diaclone, France. Cell proliferation BrdU ELISA assay was purchased from MERCK, Germany. Ethanol 96% (EtOH) was

purchased from Carlo Erba, France. Rabbit anti-human phospho-p44/42 MAPK (ERK1/2), rabbit anti-human p44/42 MAPK (ERK1/2), goat anti-rabbit IgG Alexa Fluor 488 conjugate, and rabbit IgG isotype antibodies (mAb) were purchased from Cell Signaling Technology. Fluoromount G was purchased from Southern Biotech.

**2.3. Preparation of the  $\gamma$ -Irradiated Blended Fibroin/Aloe Gel Extract Film.** Fibroin from silk cocoon (*Bombyx Mori*, Nang-Laai strain) and aloe gel extract from the gel part of the *aloe vera* (*Aloe barbadensis* miller) leaf were extracted separately to achieve the lyophilized form. Subsequently, they were qualified to control the physicochemical characteristics prior to the preparation of the film according to our previous study.<sup>12,13,20</sup> The obtained fibroin commonly provided a percentage of yield in the range of 54–58% w/w and protein content in the range of  $97.43 \pm 0.44\%$  w/w. For the infrared spectra obtained using Fourier transform infrared (FTIR) spectroscopy, amide I at 1611–1696, amide II at 1501–1550, and amide III at 1200–1320  $\text{cm}^{-1}$  must be found. Moreover, its molecular weight pattern would consist of a band of L-chain at 25 kDa and a smear band of H-chain in the range of 30–245 kDa. For aloe gel extract, it generally provided a percentage of yield in the range of 0.04–0.06% w/w and protein content in the range of  $6.86 \pm 1.15\%$  w/w. The infrared (IR) spectra of the aloe gel extract indicated peaks at 1730–1740 and 1236–1252 (O-acetyl ester), 1030–1079 (glucan units), 875–959 (pyranoside ring), and 805–813 (mannose)  $\text{cm}^{-1}$ . The molecular weight pattern presented bands of 14 and 20–100 kDa.

The film preparation was performed as in our previous study.<sup>20</sup> Briefly, 540 mg of lyophilized fibroin and 15 mg of lyophilized aloe gel extract were dissolved for 1 h in lactic acid solution (pH  $4.0 \pm 0.2$ ), finalizing volume of 15 mL. The mixed extract solution was then filtered and cast in a square-shaped mold ( $6 \times 6 \text{ cm}^2$ ) at  $47 \pm 2 \text{ }^\circ\text{C}$  for 4 h, as shown in Figure 1. The ratio of the blended fibroin to aloe gel extract in the film ( $36 \text{ cm}^2$ ) was 97.3 to 2.7% w/w. For sterilization, the obtained film was performed using a  $\gamma$  irradiation technique facilitated by Thai Adhesive Tapes Industry, Ltd., Bangkok, Thailand. Subsequently, the physicochemical properties of the sterilized film was determined to control the quality, including physical appearance (flexible yellowish film with an approximate thickness of 0.05 mm), nonporous morphology by scanning electron microscopy (SEM) imaging, and mechanical properties (breaking force of  $6.26 \pm 0.44 \text{ N}$  and percentage elongation at break of  $1.20 \pm 0.07\%$ ). For the chemical structure analysis, FTIR spectroscopy presented infrared spectra at 1630–1640 (amide I), 1510–1520 (amide II), 1220–1240 (amide III), 1050–1060 (glucan units), 1010–1020 (pyranoside ring), and 820–830 (mannose)  $\text{cm}^{-1}$ .

**2.4. Film Extract Preparation.** The film extract named in the present study was the film-free supernatant collected from incubating  $1 \times 1 \times 0.005 \text{ cm}^3$  of sterilized film in 1 mL of serum-free DMEM at  $37 \text{ }^\circ\text{C}$  for 24 h. The collected supernatant was filtered and used in further experiments.

**2.5. Fibroblast Cell Culture.** Fibroblasts used in this study were classified into three groups: normal dermal fibroblasts (NDF), diabetic dermal fibroblasts (DDF), and diabetic wound fibroblasts (DWF). NDF and DWF were, respectively, obtained from one patient undergoing skin abdominal plastic surgery and one patient with diabetic foot ulcers. The isolation and culture methods of fibroblasts were consistent with previous reports.<sup>21</sup> DDF were purchased from PELOBIOTECH GmbH, Germany.

Cells were cultured in complete DMEM supplemented with 10% FBS and 1% PS (10,000 U/mL penicillin, and 10 mg/mL

streptomycin) at  $37 \text{ }^\circ\text{C}$  in a humidified 5%  $\text{CO}_2$  atmosphere. Cells were trypsinized when they reached a confluency of 80% and used up to passage 8.

**2.6. Cytocompatibility and Cell Proliferation.** The fibroblast cells ( $1 \times 10^4$  cells/well) were cultured in a 96-well plate for 24 h. The incubated medium was replaced with DMEM with FBS-free (0% FBS), DMEM with 2% FBS, and DMEM with the film extract, and incubation was conducted for 24 h. The incubated medium was replaced with 100  $\mu\text{L}$  of serum-free DMEM containing MTT reagent (0.5 mg/mL) for 4 h, and then, 100  $\mu\text{L}$  of DMSO was added to each well. The absorbance was read at 517 nm using a spectrophotometer (Multiskan FC, Thermo Scientific). The experiment was performed in triplicates ( $n = 8$ ) for each condition. Additionally, for each group, the percentage of viability of the control (DMEM with 0% FBS) has been adjusted as 100% and compared with the other two conditions (DMEM with 2% FBS and DMEM with the film extract).

The cell proliferation was quantified by a BrdU assay kit according to the manufacturer's protocol. Briefly, fibroblast cells ( $1 \times 10^4$  cells/well) were seeded in a 96-well plate and incubated for 24 h. The incubated medium was replaced by DMEM with 0% FBS, DMEM with 2% FBS, and DMEM with film extract for 24 h. BrdU labeling solution (100  $\mu\text{L}$ ) was added and incubated at  $37 \text{ }^\circ\text{C}$  for 24 h. After the incubation, the solution was removed and 200  $\mu\text{L}$  of FixDeant was added and incubated at room temperature (RT) for 30 min. Then, 100  $\mu\text{L}$  of the anti-BrdU-POD working solution was added and incubated at RT for 2 h. The solution was removed and washed three times with 100  $\mu\text{L}$  of PBS. After the washing, 100  $\mu\text{L}$  of substrate solution was added and incubated at RT for 10 min, followed by 25  $\mu\text{L}$  of 1 M sulfuric acid. The absorbance at 450 nm was detected using a spectrophotometer. The experiment was performed in triplicates ( $n = 8$ ) per condition. Additionally, for each group, the percentage of cell proliferation of the control (DMEM with 0% FBS) was adjusted to 100% and compared with the other two conditions (DMEM with 2% FBS and DMEM with film extract).

**2.7. Cell Cycle.** Fibroblast cells ( $1 \times 10^5$  cells/well) were seeded in a 6-well plate for 24 h. The incubated medium was replaced by DMEM with 0% FBS, DMEM with 2% FBS, and DMEM with film extract for 24 h. After incubation, supernatants were discarded and cells were detached with 0.25% trypsin/0.01 M EDTA. Cell suspensions were centrifuged, and pellets were then fixed with 70% EtOH at  $4 \text{ }^\circ\text{C}$  overnight. After being washed with cold PBS, cell pellets were stained with 300  $\mu\text{L}$  of PBS + 5  $\mu\text{L}$  of PI (from 50  $\mu\text{g}/\text{mL}$  stock solution) + 1  $\mu\text{L}$  of RNase (from 100  $\mu\text{g}/\text{mL}$  stock solution). The cell cycle was analyzed using an LSR Fortessa flow cytometer (Becton Dickinson). The experiment was performed in triplicate ( $n = 3$ ) per condition. The percentage of total cells for each cell cycle phase (G0/G1, S, and G2/M) and for each cell group was reported.

**2.8. Cell Migration.** Fibroblast cells ( $3 \times 10^4$  cells/well) were seeded in 96-well ImageLock plates. When the cells reached the confluent monolayer, the IncuCyte Wound Marker tool (Sartorius, Germany) was utilized to create a scratching area. Cells were washed gently with PBS, followed by adding DMEM with 0% FBS, DMEM with 2% FBS, and DMEM with film extract for 24 h and incubated in the IncuCyteS3 system (Sartorius, Germany). To record cell migration, the scratched areas were photographed immediately after scratching in real time every 2 h over a period of 48 h. Relative wound density was quantified using the IncuCyte Software S3 (Sartorius), measuring the spatial cell density in the wound area relative to

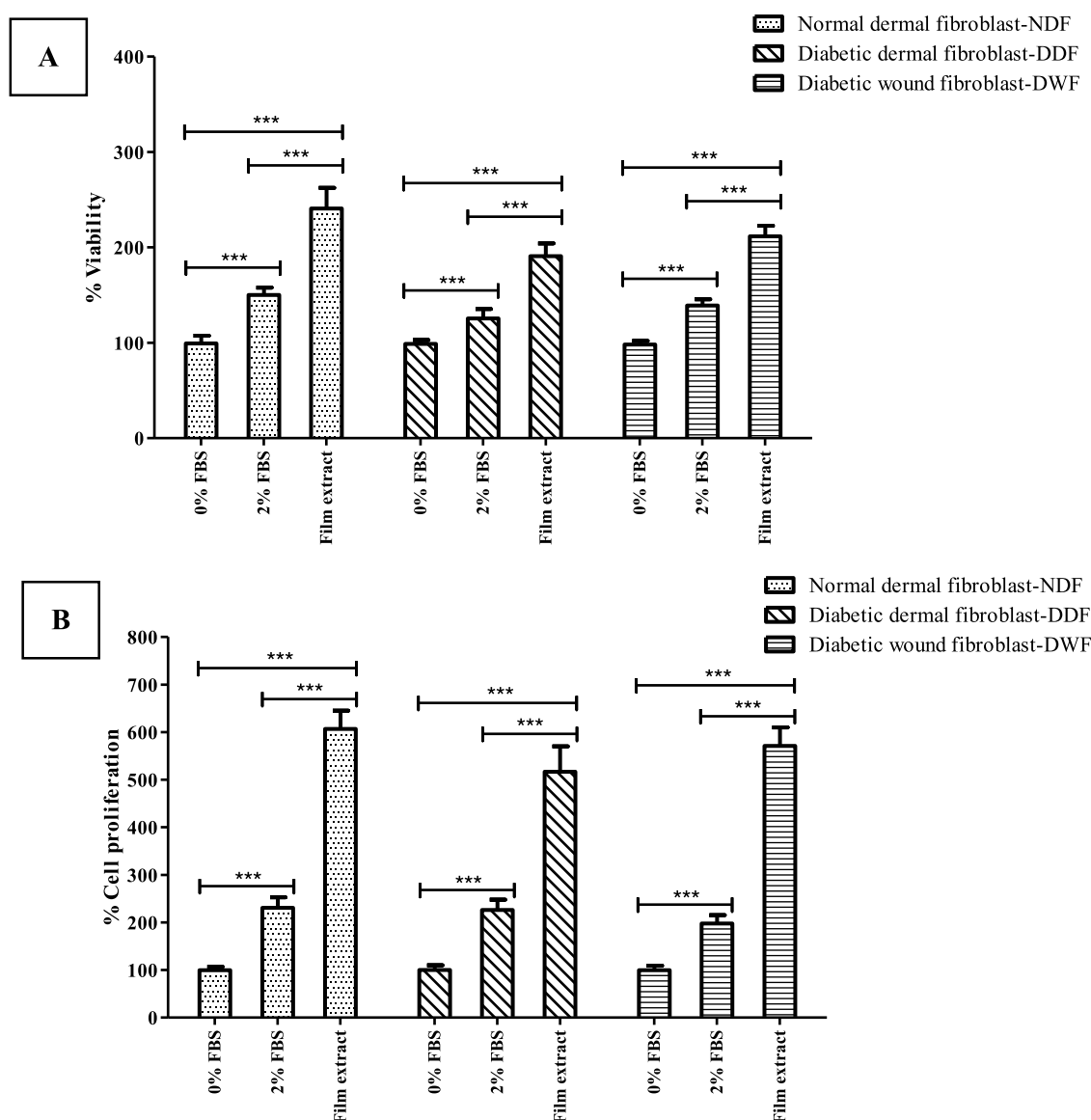


**Figure 2.** Determination of (A) viability and (B) proliferation of fibroblasts (NDF, DDF, and DWF) cultured with DMEM with 0% FBS, DMEM with 2% FBS, and DMEM with film extract for 24 h. Cell viability and cell proliferation were measured using XTT assay and BrdU assay. Data for individual cell types are expressed as the percentage of the control group (FBS-free DMEM), which is considered as 100% cell viability and cell proliferation; each column represents mean  $\pm$  S.D. in triplicate ( $n = 8$ ); \*\*\*  $p < 0.001$ .

the spatial cell density outside of the wound area at every time point. The experiment was performed in triplicate ( $n = 5$ ) per condition.

**2.9. Cell Senescence.** Fibroblast cells ( $1 \times 10^4$  cells/well) were seeded in a 96-well plate for 24 h. The incubated medium was replaced by DMEM with 0% FBS, DMEM with 2% FBS, and DMEM with film extract for 24 h. The SA- $\beta$ -galactosidase (SA- $\beta$ -gal) activity was quantified by the senescence cells histochemical staining kit according to the manufacturer's protocol. Briefly, cells were fixed for 5 min at RT and incubated with SA- $\beta$ -gal staining solution at 37 °C overnight (without CO<sub>2</sub> atmosphere). They were counterstained with the DAPI solution (5  $\mu$ L/mL) for 10 min at RT. The SA- $\beta$ -gal positive cells exhibited a blue color. Three independent fields were randomly selected in each well to observe cells. Cells were scored by bright-field and fluorescence microscopy (Olympus IX50 microscope, Japan). Data were expressed as the ratio percentage

of SA- $\beta$ -gal positive cells to the total cell count. The experiment was performed in triplicate ( $n = 8$ ) per condition.

**2.10. VEGF Protein Secretion.** Fibroblast cells ( $2 \times 10^5$  cells/well) were seeded in a 12-well plate and incubated for 24 h. The incubated medium was replaced by DMEM with 0% FBS, DMEM with 2% FBS, and DMEM with film extract for 24 h. Supernatants were collected with 10% v/v anti-protease solution. The concentration of VEGF from the supernatant was assessed using a VEGF ELISA kit following the manufacturer's protocol. Briefly, 50  $\mu$ L of assay solution was added, followed by 200  $\mu$ L of standards or cell culture supernatant, and incubated at RT for 2 h. Then, 200  $\mu$ L of human VEGF-conjugated antibody was added and incubated at RT for 2 h. After washing, 200  $\mu$ L of substrate solution was added and incubated at RT for 30 min. The reaction was stopped with 50  $\mu$ L of stop solution. Then, absorbance was measured at 450 nm using a spectrophotometer. The amount of VEGF was expressed in pg/mg protein. The protein content was

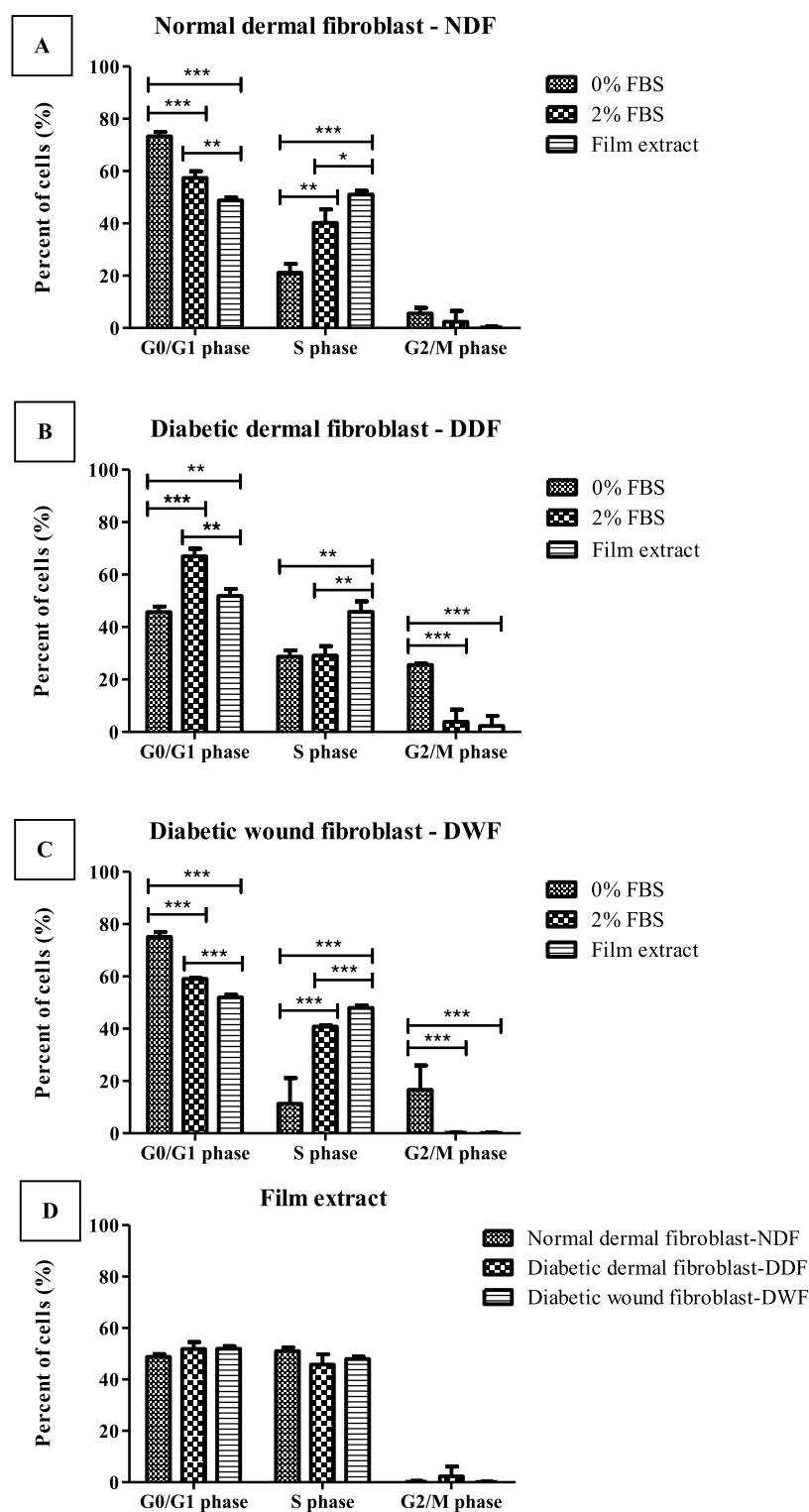


**Figure 3.** Cell cycle phases of fibroblasts (NDF, DDF, and DWF) cultured with DMEM with 0% FBS, DMEM with 2% FBS, and DMEM with film extract for 24 h. The cell cycle was analyzed by flow cytometry. The figures show the percentage of total cells in the G0/G1 phase, S phase, and G2/M phase of (A) NDF, (B) DDF, and (C) DWF and (D) the effect of DMEM with film extract in different cell types. Each column represents mean  $\pm$  S.D. in triplicate ( $n = 4$ ); \*  $p < 0.05$ , \*\*  $p < 0.01$ , and \*\*\*  $p < 0.001$ .

determined by the Bradford assay with BSA as the protein standard. The experiment was performed in triplicate ( $n = 4$ ) per condition.

**2.11. ERK1/2 Signaling Pathway Assays. 2.11.1. Cell Culture and MEK/ERK Inhibitor Treatment.** NDF were cultured for 24 h in a complete DMEM, which was changed

during 1 h for serum-free DMEM with or without the PD98059 solution ( $10 \mu\text{M}$ ), followed by 24 h of incubation in DMEM with 0% FBS, DMEM with 2% FBS, and DMEM with film extract. Cell proliferation was quantified by the BrdU assay kit described above. The experiment was performed in triplicate ( $n = 8$ ) per condition.

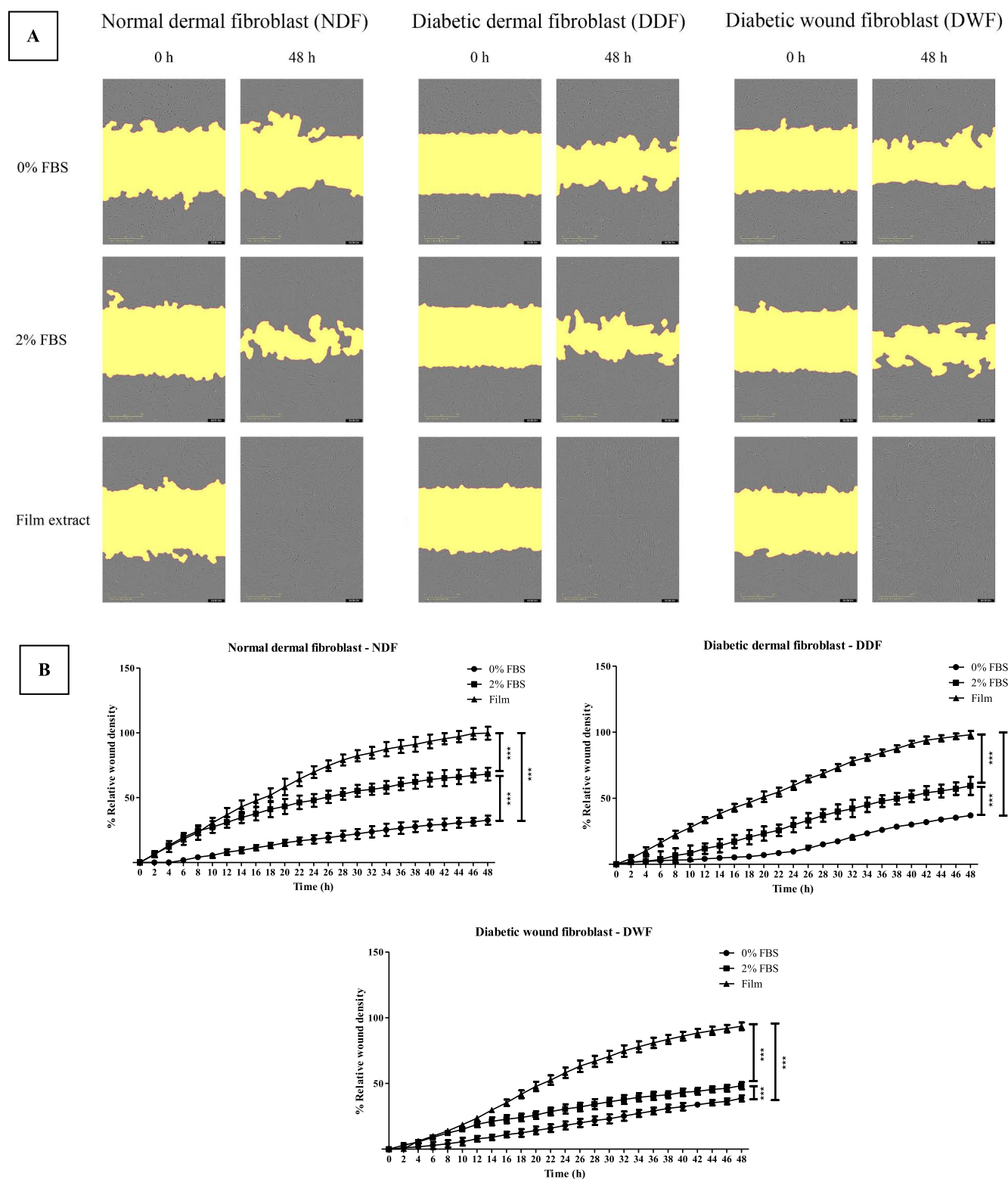


**Figure 4.** Migration of fibroblasts (NDF, DDF, and DWF) cultured with DMEM with 0% FBS, DMEM with 2% FBS, and DMEM with film extract for 48 h. Cell migration was studied by the scratch assay. The figures demonstrate (A) the visualization of the scratching gap at 10 $\times$  magnification and (B) the percentage of relative wound density. Each time point represents mean  $\pm$  S.D. in triplicate ( $n = 5$ ); \*\*\*  $p < 0.001$  at 48 h.

**2.11.2. Confocal Imaging.** NDF ( $1 \times 10^5$  cells/well) were seeded onto coverslips in a 12-well plate for 24 h. The incubated medium was replaced by 10  $\mu$ M of PD98059 for 1 h. The cells were then washed and incubated in DMEM with 0% FBS, DMEM with 2% FBS, and DMEM with film extract for 1 and 24

h. They were then fixed with paraformaldehyde (PFA 4% final concentration in PBS) at RT for 10 min, washed, permeabilized using 0.1% Triton X-100 for 10 min, washed, and blocked with 5% goat serum + 0.3% Triton X-100 in PBS for 1 h at 4  $^{\circ}$ C. Coverslips were incubated with phospho-p44/42 MAPK

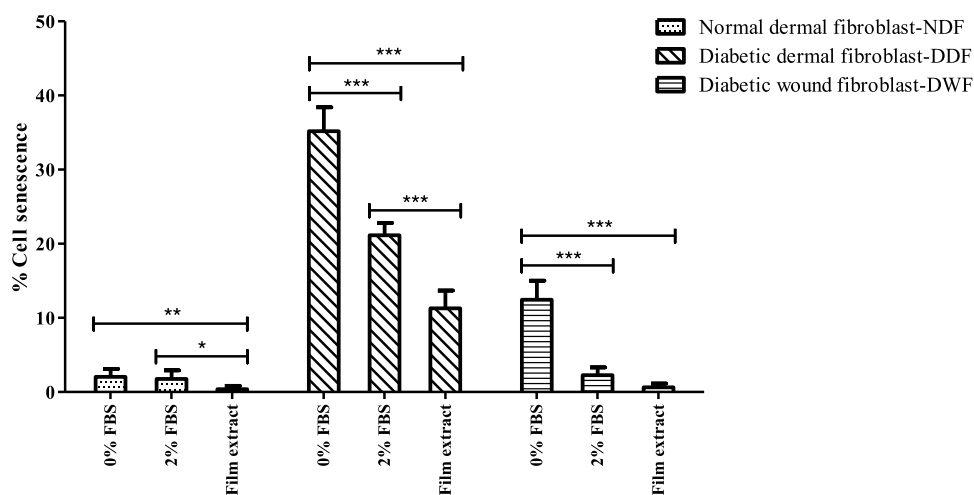


**Figure 5.** Senescence of fibroblasts (NDF, DDF, and DWF) cultured with the DMEM with 0% FBS, DMEM with 2% FBS, and DMEM with film extract for 24 h. The cell senescence was quantified using the SA- $\beta$ -gal activity assay. Data are expressed as the ratio percentage of SA- $\beta$ -gal positive cells to the total cell count, each column represents mean  $\pm$  S.D. in triplicate ( $n = 8$ ); \*  $p < 0.05$ , \*\*  $p < 0.01$ , and \*\*\*  $p < 0.001$ .

(ERK1/2) (Thr202/Tyr204) XP rabbit mAb (1:200 in diluent (PBS with 1% BSA + 0.3% Triton X-100)) in a humidified chamber at 4 °C for overnight. The cells were washed and then incubated with goat anti-rabbit IgG Alexa Fluor 488-conjugated secondary antibody (1:100 in diluent) for 1 h at 4 °C. They were washed and stained with DAPI to visualize nuclei. Coverslips were mounted with Fluoromount reagent. The immunofluorescence images were captured with an LSM 800 laser scanning confocal microscope (Zeiss, Germany).

**2.11.3. Flow Cytometry.** NDF ( $6 \times 10^5$  cells/well) were cultured in a 12-well plate for 24 h. The supernatant was then discarded and replaced with DMEM with 0% FBS, DMEM with 2% FBS, and DMEM with film extract for 24 h. After incubation, the cells were detached and fixed with 4% PFA at RT for 10 min. After washing, the cells were permeabilized with 0.1% Triton X-100 at RT for 15 min. They were then suspended in blocking buffer containing 5% goat serum + 0.3% Triton X-100 in PBS for 1 h at 4 °C and incubated overnight at 4 °C with p44/42 MAPK (ERK1/2) rabbit mAb (1:400 in diluent), phospho-p44/42 MAPK (ERK1/2) (Thr202/Tyr204) XP rabbit mAb (1:800 in diluent) and rabbit mAb Isotype control (1:200 in diluent). After washing, the cells were incubated with goat anti-rabbit IgG Alexa Fluor 488 conjugate (1:100 in diluent) in the dark at 4 °C for 1 h. Finally, the cells were washed, suspended in 2 mM EDTA/PBS, and analyzed using a flow cytometer (LSR Fortessa, Becton Dickinson). FACS analysis was performed using FACSDiva software (Becton Dickinson); 20,000 events were recorded for each sample. The results are mean values of fluorescence intensity  $\pm$  SD of triplicate measurements ( $n = 4$ ) per condition.

**2.12. Statistical Analysis.** The data are presented as the mean  $\pm$  SD. Statistical comparisons between each condition were performed using a one-way ANOVA test (GraphPad Prism software).

### 3. RESULTS

**3.1. Cytotoxicity and Cell Proliferation.** For the cytotoxicity, the results showed that NDF, DDF, and DWF treated with film extract for 24 h have viability percentages of  $242.77 \pm 8.95$ ,  $193.24 \pm 6.91$ , and  $215.52 \pm 5.22$ , respectively, which are significantly higher than DMEM with 0% FBS ( $100 \pm 8.34$ ,  $100 \pm 4.21$ , and  $100 \pm 3.79$ ) and DMEM with 2% FBS

( $151.26 \pm 5.12$ ,  $127.15 \pm 7.83$ , and  $141.64 \pm 4.69$ ), as shown in Figure 2A. In the proliferation assay, Figure 2B illustrates that NDF, DDF, and DWF treated with film extract for 24 h have proliferation percentages of  $608.83 \pm 6.39$ ,  $515.42 \pm 10.26$ , and  $576.90 \pm 6.87$ , respectively, which are significantly higher than DMEM with 0% FBS ( $100 \pm 7.35$ ,  $100 \pm 9.54$ , and  $100 \pm 9.37$ ) and DMEM with 2% FBS ( $231.49 \pm 9.73$ ,  $225.63 \pm 9.51$ , and  $198.30 \pm 9.02$ ).

**3.2. Cell Cycle.** The effect of the film extract on the fibroblast cell cycle as the percentage of cells in cell cycle phases (G0/G1, S, and G2/M) was determined. The percentage of NDF in the G0/G1 phase was significantly lower with film extract ( $48.76 \pm 1.15$ ) than with DMEM with 0% FBS ( $73.80 \pm 1.65$ ) and DMEM with 2% FBS ( $57.38 \pm 2.54$ ), whereas, in the S phase, the percentage of NDF was significantly higher with film extract ( $51.03 \pm 1.45\%$ ) compared to DMEM with 0% FBS ( $21.12 \pm 3.40\%$ ) and DMEM with 2% FBS ( $40.22 \pm 5.12\%$ ), as shown in Figure 3A. The same trend was observed for DDF and DWF; the percentage of NDF in the S phase was significantly higher with film extract ( $45.81 \pm 3.98\%$ ,  $47.92 \pm 0.93\%$ , respectively) compared to DMEM with 0% FBS ( $28.72 \pm 2.43\%$ ,  $11.28 \pm 9.82\%$ ) and DMEM with 2% FBS ( $29.12 \pm 3.60\%$ ,  $40.78 \pm 0.50\%$ ) (Figure 3B,C). Figure 3D also indicates the effect of the film extract in different cell types as the percentage of total cells in each cell cycle phase. The data showed that the percentage of total cells for each cell cycle phase was not significantly different in each cell type.

**3.3. Cell Migration.** Cell migration was studied by the IncuCyte scratch assay modified by An et al.<sup>22</sup> The results showed that NDF, DDF, and DWF treated with film extract for 24 h elucidated a completely healed scratch after 48 h, while under other conditions (DMEM with 0% FBS and DMEM with 2% FBS), they exhibit no wound closure at the same time, as shown in Figure 4A. At 48 h, percentages of relative wound density for NDF, DDF, and DWF treated with film extract were  $99.73 \pm 5.01$ ,  $98.01 \pm 2.90$ , and  $93.47 \pm 2.86\%$ , respectively, which reached approximately 100% of relative wound density, whereas they were lower for NDF, DDF, and DWF cultured with DMEM with 0% FBS ( $32.65 \pm 3.52$ ,  $37.01 \pm 1.75$ , and  $38.63 \pm 2.36\%$ ) and DMEM with 2% FBS ( $68.15 \pm 4.91$ ,  $59.37 \pm 6.85$ , and  $48.27 \pm 2.71\%$ ) (Figure 4B).

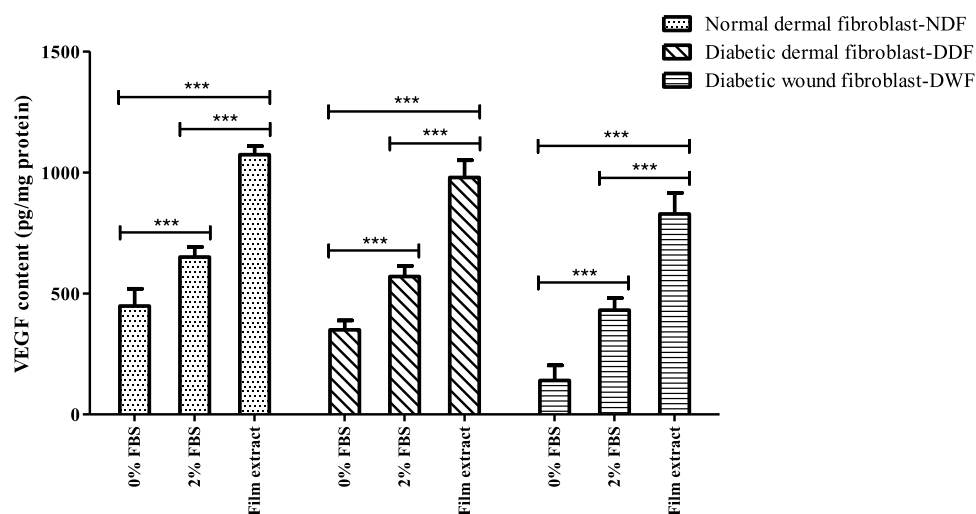


**Figure 6.** Determination of VEGF secretion by fibroblasts (NDF, DDF, and DWF) cultured with DMEM with 0% FBS, DMEM with 2% FBS, and DMEM with film extract for 24 h. The level of VEGF was assessed by the VEGF ELISA colorimetric assay. Data are expressed as the VEGF content (pg/mg protein), and each column represents mean  $\pm$  S.D. in triplicate ( $n = 4$ ); \*\*\*  $p < 0.001$ .

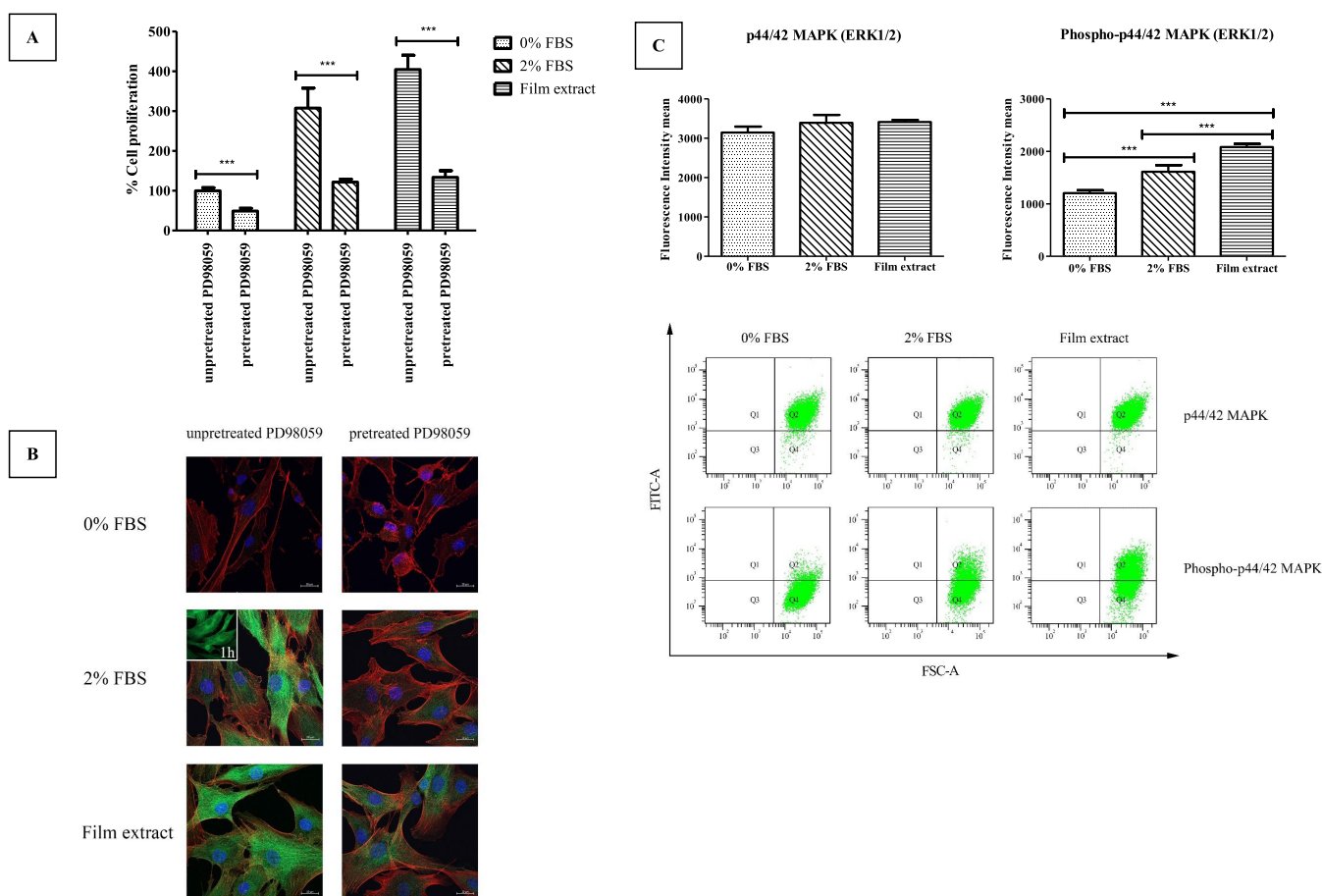


**Figure 7.** Investigation of the ERK1/2 activity in normal dermal fibroblast cultured with DMEM with 0% FBS, DMEM with 2% FBS, and DMEM with film extract for 24 h. (A) The inhibitory effect of nonpretreatment or pretreatment with 10  $\mu$ M of PD98059 solution (MEK/ERK inhibitor) for 1 h on the cell proliferation, which was quantified by the BrdU assay; data are expressed as the percentage of the control group (DMEM with 0% FBS unpretreated with PD98059) considered as 100% cell proliferation; each column represents mean  $\pm$  S.D. in triplicate ( $n = 8$ ); \*\*\*  $p < 0.001$ . (B) Immunofluorescence images of phospho-p44/42 protein (green), F-actin (red), and nucleus (blue) by confocal microscopy (40 $\times$  objective magnification). Box area at 1 h after DMEM 2% FBS culture; bars: 20  $\mu$ m. (C) The quantitative flow cytometry analysis with plots and histograms identifying p44/42 MAPK (ERK1/2) and phospho-p44/42 MAPK (ERK1/2) protein levels, each column of the histograms represents mean  $\pm$  S.D. in triplicate ( $n = 4$ ); \*\*\*  $p < 0.001$ .

**3.4. Cell Senescence.** The film extract contributed to significantly inhibiting the percentage of cell senescence in NDF, DDF, and DWF as  $0.39 \pm 0.43$ ,  $11.30 \pm 2.39$ , and  $0.63 \pm 0.51\%$ , respectively, compared to DMEM with 0% FBS ( $2.04 \pm 1.09$ ,  $35.18 \pm 3.22$ , and  $12.43 \pm 2.57\%$ ) and DMEM with 2% FBS ( $1.77 \pm 1.16$ ,  $21.15 \pm 1.67$ , and  $2.27 \pm 1.03\%$ ), as shown in Figure 5.

**3.5. VEGF Secretion.** Figure 6 illustrates that NDF, DDF, and DWF treated with film extract for 24 h secrete significantly higher levels of VEGF ( $1072 \pm 35.85$ ,  $979.28 \pm 70.97$ , and  $828.24 \pm 87.33$  pg/mg protein, respectively) than those treated with DMEM with 0% FBS ( $448.06 \pm 70.96$ ,  $349.62 \pm 39.20$ , and  $140.59 \pm 62.68$  pg/mg protein) and DMEM with 2% FBS ( $650.51 \pm 41.41$ ,  $569.87 \pm 43.77$ , and  $430.69 \pm 50.26$  pg/mg protein).

**3.6. MAPK/ERK Pathway.** Whatever the culture condition (DMEM with 0% FBS, DMEM with 2% FBS, film extract), the pretreatment for 1 h with the PD98059 suppressed cell proliferation and phospho-p44/42 MAPK (ERK1/2) expression, as shown in Figure 7A,B. For the quantitative flow cytometry data on p44/42 MAPK (ERK1/2) phosphorylation, we found that the film extract activates the phospho-p44/42 MAPK (ERK1/2), confirmed by immunofluorescence images shown in Figure 7B. The mean fluorescence intensity value of phospho-p44/42 MAPK (ERK1/2) was significantly higher with the film extract ( $2082.50 \pm 41.41$ ) than with DMEM with 0% FBS ( $1206.00 \pm 56.23$ ) and DMEM with 2% FBS ( $1611.50 \pm 126.74$ ), as shown in Figure 7C.

## 4. DISCUSSION

The wound healing process is usually delayed or impaired for patients under diabetic conditions. A major chronic complication is diabetic foot ulcers. A diabetic environment could be associated with dermal fibroblast dysfunction, reduced angiogenesis, the release of proinflammatory cytokines, and senescence features. Alternative therapeutic treatments using natural products are highly demanded for their high potential of bioactive activity in skin repair. We developed a dressing comprising silk fibroin and *Aloe vera* gel extract for a novel approach to the treatment of chronic wound pathologies. Previously, the main markers during the wound healing process were investigated. This study aimed to elucidate the possible MAPK/ERK signaling pathway related to the biological effects of the dressing on fibroblast cells. This investigation was conducted on NDF, DDF, and DWF for the cellular responses and on NDF for the MAPK/ERK signaling pathway.

The cytotoxicity of fibroblasts was evaluated using the MTT colorimetric assay, which provides a readout of cell viability and growth by measuring the metabolic activity of any viable or proliferative cells with NADPH-dependent enzymes that reduce MTT. These results implied that the film extract behaved as having a noncytotoxicity effect on fibroblast cells and might also have the potential to stimulate cell viability and proliferation. Also, the results were similar to our previous study.<sup>20</sup>

The quantification of cell proliferation of fibroblast cells was performed using the colorimetric BrdU assay. This quantification of cell proliferation is based on the measurement of the incorporation of BrdU (bromodeoxyuridine is a synthetic nucleoside, a structural analogue of thymidine) during DNA synthesis. The results were related to cell viability, which implied a higher rate of cell viability as a higher rate of cell proliferation. In the hyperglycemic environment, the declined cell proliferation is caused by several issues such as the increase of L-lactate

secretion, proinflammatory mediators, and advanced glycation end-products (AGE), leading to enhanced apoptosis *via* activation of ROS, proapoptotic transcription factor FOXO1, and caspase.<sup>23</sup> As the outcome, the film extract is composed of factors that enhance cell proliferation, which is concurrent to the previous findings. As its remarkable properties, silk fibroin regulates the NF- $\kappa$ B signaling pathway and expression of proteins involved in cell proliferation, including vimentin, cyclin D1, VEGF, and fibronectin.<sup>24</sup> Two fibroin-derived peptides, VITTDSDGNE and NINDFDED, located in the N-terminal region, were identified as active agents targeting fibroblast growth.<sup>25</sup> Also, a 29 kDa glycoprotein displayed the potential to stimulate the proliferative activity of kidney cells in hamsters and human dermal fibroblasts.<sup>26</sup> Moreover, acemannan is one of the main polysaccharide compounds of *Aloe vera*, providing synergistic effects to promote cell proliferation and skin wound healing through the AKT/mTOR signaling pathway.<sup>27</sup>

Stain DNA with PI and flow cytometry experiments were performed for cell cycle analysis. Typically, p21<sup>Cip1</sup> and p27<sup>Kip1</sup> are the cyclin-dependent kinase (CDK) inhibitors (CKIs) that play an essential role in interfering with the kinase activities related to the cell cycle. These CKIs are significantly elevated at high glucose levels and inhibit the cyclin/CDK complexes. In cell cycle progression, cells are arrested in the G1 phase, and the proliferation rate is restricted, followed by impaired wound healing processes.<sup>28</sup> As the depicted cell cycle data implies, the film-treated cells shifted from the G0/G1 phase to the S phase by binding to cyclin D/CDK4,6 complexes that regulate G1-S phase transit. The film extract promoted cells to enter the S phase *via* the pathway of acemannan, which is an important stage for mitosis and cell growth by influencing cyclin-dependent cell cycle progress through translational regulation of cyclin D1.<sup>20</sup> Our cell cycle finding was liable to Yuan et al. who reported that after treating with aloe polysaccharide, the number of cells was increased in the S and G2/M phases preparing for mitosis, and cyclin D1 protein was upregulated in a concentration-dependent manner.<sup>29</sup> Thus, we hypothesized that the film extract stimulates cyclin D1 expression in cultured fibroblasts and functions as a transcriptional coregulator ensuing to initiate the shift from cell arrest (G0/G1 phase) to cell synthesis (S phase).

Cell migration was studied by the IncuCyte scratch assay. Regarding the hyperglycemic condition, the excessive production of ROS led to their accumulation, resulting in protein structure dysfunction and aberration of cell migration directly by over-activation of the small Rho GTPase Rac1, thus affecting the cell polarity and morphology.<sup>3</sup> Following the effect of film extract to promote cell migration was coincident with the study on mouse embryonic fibroblasts and damaged skin rats, which showed that silk fibroin stimulates the pathway of canonical NF- $\kappa$ B signaling, which is associated with fibroblast migration and the wound healing process.<sup>24</sup> Moreover, a 5.5 kDa glycoprotein isolated from the *Aloe vera* gel improved cell proliferation and migration using keratinocyte scratch wound monolayer.<sup>30</sup>

SA- $\beta$ -gal staining was used to measure senescence, a regulatory cell response to multiple types of cellular stress leading to the permanent cell-cycle arrest. The process of cell cycle arrest is regulated by activating p53/p21<sup>CIP1</sup> and p16<sup>INK4a</sup>/Rb tumor suppression pathways.<sup>31</sup> Under diabetic conditions, several downstream cellular abnormalities, especially for cutaneous fibroblasts, are present *via* enhanced activation of p53/p21-dependent pathways and increased senescence-associated  $\beta$ -galactosidase (SA- $\beta$ -gal) activity, resulting in cell senescence and wound healing dysfunction.<sup>32</sup> Thus, cell

senescence can compromise tissue repair and regeneration. In this study, the film extract contributed to significant inhibition of fibroblast senescence. These data corresponding to Ma et al. reported that fibroin improved the osseointegration of porous titanium implants under diabetic conditions *via* activation of the PI3K/Akt signaling pathway.<sup>33</sup> Also, Hu et al. found that polysaccharides and flavonoids contained in *Aloe vera* possess free radical scavenging activity.<sup>34</sup> We suggested that the film extract has a protective effect on cellular senescence by regulating ROS-induced stress pathways.

The production of VEGF by fibroblasts induces angiogenesis by stimulating the formation of blood vessels and the expansion of an existing vascular bed as it acts as a highly specific mitogen for endothelial cells.<sup>35</sup> It is, therefore, one of the essential mediators associated with the wound healing process. VEGF secretion was determined by a colorimetric ELISA kit. An impaired glucose tolerance condition leads to the malfunction of VEGF expression, resulting in cell proliferation and cell migration disturbances, and also affects the prolonged wound healing rate.<sup>36</sup> These results confirmed that the film extract could improve the skin repair process by stimulating VEGF secretion. The increase of VEGF secretion was interrelated to the finding of acetyl groups in acemannan and its derivatives, and the  $\beta$ -sitosterol compounds of *Aloe vera* have been investigated to be essential stimulators of VEGF expression.<sup>37</sup> Additionally, *Aloe vera* likewise upregulated the expression of the VEGF gene in the diabetes-induced rats.<sup>8</sup>

In summary, whatever the origin of fibroblasts including NDF, DDF, and DWF, we demonstrated that the film extract enhances cell proliferation and migration, stimulates VEGF secretion, and prevents cell senescence features. All of these results suggested that the blended fibroin/alginate gel extract film has significant effects on wound healing. Next, we selected NDF to elucidate the underlying mechanism, particularly the principal intracellular signaling pathway targeted by the film extract.

MAPK pathways are the primary key driving signaling events that facilitate wound healing processes, including cell proliferation, cell migration, cell differentiation, and angiogenesis.<sup>38</sup> Activation of MAPK complexes regulates transcription factors by phosphorylating downstream proteins and finally initiates cell proliferation and differentiation signals to the nucleus. In this study, to investigate the biomolecular mechanism(s) of the film extract, we focused on three MAPK signaling pathways, including ERK, JNK, and p38, which play a major role in the development of nonhealing wound pathologies such as DFU. We used confocal microscopy imaging of immunofluorescence-labeled NDF over different time points (1, 4, 18, and 24 h) to reveal the abundance of ERK1/2, JNK1/2, and p38-MAPK phosphoproteins. We observed that film extract leads to higher levels of ERK1/2 phosphorylation compared to JNK1/2 and p38-MAPK (data not shown). So, we further investigated more precisely the effect of the film extract on the MAPK/ERK pathway, focusing on phospho-p44/42 MAPK (ERK1/2), a transcription factor related to cell proliferation. The activation of the MAPK/ERK cascade can be stimulated *via* various factors, including (1) a variety of growth factors and cytokines; (2)  $\text{Ca}^{2+}$  influx; (3) activation of receptor tyrosine kinase Ras, protein kinase-mediated, G-protein-coupled receptor ligands; and (4) membrane depolarization.<sup>39</sup> We utilized the PD98059 inhibitor, a flavonoid compound considered as a potent inhibitor of MEK/ERK1/2 cascade by binding to MEK/ERK1/2, inducing an inactive MEK/ERK1/2 form and preventing the activation of the upstream activator (c-Raf).<sup>40</sup> For the effect of the MEK/

ERK1/2 inhibitor, these results confirmed the positive correlation between the level of MAPK (ERK1/2) activity and the cellular growth rate. They also indicated the direct effect of FBS and film extract on cell proliferation, mediated by the MAPK/ERK pathway. Regarding the quantitative flow cytometry data on p44/42 MAPK (ERK1/2) phosphorylation, the film extract can activate the phospho-p44/42 MAPK (ERK1/2) confirming immunofluorescence images. The confocal microscopy images allowed the detection and localization of intracellular MAPK/ERK activity. The green fluorescent staining indicated that the film extract stimulates the upregulation of phospho-p44/42 MAPK (ERK1/2), promoting downstream protein synthesis involved in the wound healing process. The obtained results were concurrent to Maemura et al. who reported that the MAPK/ERK signaling pathway promotes cell proliferation and inhibits the apoptotic cell by influencing the activity of downstream cell cycle regulatory proteins, apoptosis-related proteins, and other effector molecules, such as G1/S-specific cyclin D1.<sup>41</sup> We proposed that the film extract *via* its functional components, *Aloe vera* and fibroin, acts through the common MAPK/ERK signaling pathway. Nevertheless, according to the literature, it should regulate other signaling molecules and processes involved in dynamic signaling crosstalk, such as the NF- $\kappa$ B signaling system.<sup>42,43</sup>

Our previous clinical study indicated the wound healing efficacy of the blended fibroin/alginate gel extract film.<sup>13</sup> The film could accelerate the healing rate of diabetic foot ulcers after application for 4 weeks, implying the sufficient delivery of the bioactive compounds from the film to the wound site. In this study, to regulate the amount of the bioactive compounds released from the film, the film-free supernatant obtained from incubating the sterilized film in serum-free DMEM for 24 h (film extract) was used to clarify the molecular mechanisms of the film on the wound healing enhancer.

## 5. CONCLUSIONS

In this study, the experiments confirm and support the beneficial effects of the blended fibroin/alginate gel extract film on cell proliferation and migration, VEGF secretion, and prevention of cell senescence. The blended fibroin/alginate gel extract film displays a biological behavior with interesting properties for delayed wound healing. Its mechanism of action is mainly linked to the activation of the MAPK/ERK pathway known to regulate various cellular activities, including proliferation. Therefore, the blended fibroin/alginate gel extract film can be considered as a promising therapeutic approach in the treatment of diabetic nonhealing ulcers.

## AUTHOR INFORMATION

### Corresponding Authors

**Jarupa Viyoch** – Department of Pharmaceutical Technology, Faculty of Pharmaceutical Sciences and Center of Excellence for Innovation in Chemistry, Naresuan University, Phitsanulok 65000, Thailand; Phone: (+66)55 963730; Email: jarupav@nu.ac.th

**Céline Viennet** – UMR 1098 RIGHT INSERM EFS FC, DIMaCell Imaging Resource Center, University of Franche-Comté, Besançon 25000, France; Phone: (+33)3 83 08 22 10; Email: celine.viennet@univ-fcomte.fr

## Authors

**Preeyawass Phimmuan** – Department of Pharmaceutical Technology, Faculty of Pharmaceutical Sciences and Center of Excellence for Innovation in Chemistry, Naresuan University, Phitsanulok 65000, Thailand; UMR 1098 RIGHT INSERM EFS FC, DImaCell Imaging Resource Center, University of Franche-Comté, Besançon 25000, France; [orcid.org/0000-0003-1884-2006](https://orcid.org/0000-0003-1884-2006)

**Zélie Dirand** – UMR 1098 RIGHT INSERM EFS FC, DImaCell Imaging Resource Center, University of Franche-Comté, Besançon 25000, France

**Marion Tissot** – UMR 1098 RIGHT INSERM EFS FC, DImaCell Imaging Resource Center, University of Franche-Comté, Besançon 25000, France

**Saran Worasakwutiphong** – Division Plastic and Reconstructive Surgery, Department of Surgery, Faculty of Medicine, Naresuan University, Phitsanulok 65000, Thailand

**Anuphan Sittichokechaiwut** – Department of Preventive Dentistry, Faculty of Dentistry, Naresuan University, Phitsanulok 65000, Thailand

**François Grandmottet** – Department of Biochemistry, Faculty of Medical Science, Naresuan University, Phitsanulok 65000, Thailand

Complete contact information is available at:

<https://pubs.acs.org/10.1021/acsomega.2c07507>

## Notes

The authors declare no competing financial interest.

## ACKNOWLEDGMENTS

The authors would like to thank Naresuan University and Université Bourgogne-Franche-Comté for the support of all facilities. This work was granted from Franco-Thai scholarship under a double doctoral degree program between Naresuan University and Université Bourgogne-Franche-Comté and Global and Frontier Research University (Grant number R2566C052), Naresuan University. The authors are also thankful to the Center of Excellence for Innovation in Chemistry (PERCH-CIC), Office of the Higher Education Commission, and the Faculty of Pharmaceutical Sciences, Naresuan University for the support of all facilities.

## REFERENCES

- (1) Abid, H. M. U.; Hanif, M.; Mahmood, K.; Aziz, M.; Abbas, G.; Latif, H. Wound-healing and antibacterial activity of the quercetin-4-formyl phenyl boronic acid complex against bacterial pathogens of diabetic foot ulcer. *ACS Omega* **2022**, *7*, 24415–24422.
- (2) Edmonds, M. Diabetic foot ulcers: practical treatment recommendations. *Drugs* **2006**, *66*, 913–929.
- (3) Lamers, M. L.; Almeida, M. E. S.; Vicente-Manzanares, M.; Horwitz, A. F.; Santos, M. F. High glucose-mediated oxidative stress impairs cell migration. *PLoS One* **2011**, *6*, No. e22865.
- (4) Griffioen, A. W.; Molema, G. Angiogenesis: potentials for pharmacologic intervention in the treatment of cancer, cardiovascular diseases, and chronic inflammation. *Pharmacol. Rev.* **2000**, *52*, 237–268.
- (5) Hehenberger, K.; Kratz, G.; Hansson, A.; Brismar, K. Fibroblasts derived from human chronic diabetic wounds have a decreased proliferation rate, which is recovered by the addition of heparin. *J. Dermatol. Sci.* **1998**, *16*, 144–151.
- (6) Yamakawa, S.; Hayashida, K. Advances in surgical applications of growth factors for wound healing. *Burns Trauma* **2019**, *7*, No. s41038-019-0148-1.

(7) Demidova-Rice, T. N.; Hamblin, M. R.; Herman, I. M. Acute and impaired wound healing: pathophysiology and current methods for drug delivery, part 1: normal and chronic wounds: biology, causes, and approaches to care. *Adv. Skin Wound Care* **2012**, *25*, 304–314.

(8) Ghilardi, S. J.; O'Reilly, B. M.; Sgro, A. E. Intracellular signaling dynamics and their role in coordinating tissue repair. *WIREs Syst. Biol. Med.* **2020**, *12*, No. e1479.

(9) Awazu, M.; Ishikura, K.; Hida, M.; Hoshiya, M. Mechanisms of mitogen-activated protein kinase activation in experimental diabetes. *J. Am. Soc. Nephrol.* **1999**, *10*, 738–745.

(10) Haneda, M.; Araki, S.; Togawa, M.; Sugimoto, T.; Isono, M.; Kikkawa, R. Mitogen-activated protein kinase cascade is activated in glomeruli of diabetic rats and glomerular mesangial cells cultured under high glucose conditions. *Diabetes* **1997**, *46*, 847–853.

(11) Dhivya, S.; Padma, V. V.; Santhini, E. Wound dressings - a review. *Biomedicine* **2015**, *5*, No. 22.

(12) Inpanya, P.; Faikrua, A.; Ounaron, A.; Sittichokechaiwut, A.; Viyoch, J. Effects of the blended fibroin/alginate gel film on wound healing in streptozotocin-induced diabetic rats. *Biomed. Mater.* **2012**, *7*, No. 035008.

(13) Worasakwutiphong, S.; Termwattanaphakdee, T.; Kamolhan, T.; Phimmuan, P.; Sittichokechaiwut, A.; Viyoch, J. Evaluation of the safety and healing potential of a fibroin-alginate gel film for the treatment of diabetic foot ulcers. *J. Wound Care* **2021**, *30*, 1020–1028.

(14) Liu, T.-l.; Miao, J.-c.; Sheng, W.-h.; Xie, Y.-f.; Huang, Q.; Shan, Y.-b.; Yang, J.-c. Cytocompatibility of regenerated silk fibroin film: a medical biomaterial applicable to wound healing. *J. Zhejiang Univ., Sci., B* **2010**, *11*, 10–16.

(15) Czekay, R. P.; Wilkins-Port, C. E.; Higgins, S. P.; Freytag, J.; Overstreet, J. M.; Klein, R. M.; Higgins, C. E.; Samarakoon, R.; Higgins, P. J. PAI-1: An Integrator of Cell Signaling and Migration. *Int. J. Cell Biol.* **2011**, *2011*, No. 562481.

(16) Chantarawatit, P.; Sangvanich, P.; Banlunara, W.; Soontornvipart, K.; Thunyakitpisal, P. Acemannan sponges stimulate alveolar bone, cementum and periodontal ligament regeneration in a canine class II furcation defect model. *J. Periodontol. Res.* **2014**, *49*, 164–178.

(17) Teplicki, E.; Ma, Q.; Castillo, D. E.; Zarei, M.; Hustad, A. P.; Chen, J.; Li, J. The Effects of *Aloe vera* on Wound Healing in Cell Proliferation, Migration, and Viability. *Wounds* **2018**, *30*, 263–268.

(18) Atiba, A.; Ueno, H.; Uzuka, Y. The effect of *Aloe vera* oral administration on cutaneous wound healing in type 2 diabetic rats. *J. Vet. Med. Sci.* **2011**, *73*, 583–589.

(19) Akaberi, M.; Sobhani, Z.; Javadi, B.; Sahebkar, A.; Emami, S. A. Therapeutic effects of *Aloe* spp. in traditional and modern medicine: A review. *Biomed. Pharmacother.* **2016**, *84*, 759–772.

(20) Phimmuan, P.; Worasakwutiphong, S.; Sittichokechaiwut, A.; Grandmottet, F.; Nakyai, W.; Luangpraditkun, K.; Viennet, C.; Viyoch, J. Physicochemical and biological activities of the gamma-irradiated blended fibroin/alginate gel film. *ScienceAsia* **2022**, *48*, No. 278.

(21) Nakyai, W.; Tissot, M.; Humbert, P.; Grandmottet, F.; Viyoch, J.; Viennet, C. Effects of Repeated UVA Irradiation on Human Skin Fibroblasts Embedded in 3D Tense Collagen Matrix. *Photochem. Photobiol.* **2018**, *94*, 715–724.

(22) An, J.; Yao, W.; Tang, W.; Jiang, J.; Shang, Y. Hormesis effect of methyl triclosan on cell proliferation and migration in human hepatocyte L02 cells. *ACS Omega* **2021**, *6*, 18904–18913.

(23) Mahali, S.; Raviprakash, N.; Raghavendra, P. B.; Manna, S. K. Advanced glycation end products (AGEs) induce apoptosis via a novel pathway: involvement of Ca<sup>2+</sup> mediated by interleukin-8 protein. *J. Biol. Chem.* **2011**, *286*, 34903–34913.

(24) Park, Y. R.; Sultan, M. T.; Park, H. J.; Lee, J. M.; Ju, H. W.; Lee, O. J.; Lee, D. J.; Kaplan, D. L.; Park, C. H. NF- $\kappa$ B signaling is key in the wound healing processes of silk fibroin. *Acta Biomater.* **2018**, *67*, 183–195.

(25) Yamada, H.; Igarashi, Y.; Takasu, Y.; Saito, H.; Tsubouchi, K. Identification of fibroin-derived peptides enhancing the proliferation of cultured human skin fibroblasts. *Biomaterials* **2004**, *25*, 467–472.

- (26) Yagi, A.; Egusa, T.; Arase, M.; Tanabe, M.; Tsuji, H. Isolation and characterization of the glycoprotein fraction with a proliferation-promoting activity on human and hamster cells in vitro from *Aloe vera* gel. *Planta Med.* **1997**, *63*, 18–21.
- (27) Xing, W.; Guo, W.; Zou, C.-H.; Fu, T.-T.; Li, X.-Y.; Zhu, M.; Qi, J. H.; Song, J.; Dong, C. H.; Li, Z.; Xiao, Y.; Yuan, P. S.; Huang, H.; Xu, X. Acemannan accelerates cell proliferation and skin wound healing through AKT/mTOR signaling pathway. *J. Dermatol. Sci.* **2015**, *79*, 101–109.
- (28) Wolf, G. Cell cycle regulation in diabetic nephropathy. *Kidney Int.* **2000**, *58*, S59–S66.
- (29) Yuan, L.; Duan, X.; Zhang, R.; Zhang, Y.; Qu, M. Aloe polysaccharide protects skin cells from UVB irradiation through Keap1/Nrf2/ARE signal pathway. *J. Dermatol. Treat.* **2020**, *31*, 300–308.
- (30) Moriyama, M.; Moriyama, H.; Uda, J.; Kubo, H.; Nakajima, Y.; Goto, A.; Akaki, J.; Yoshida, I.; Matsuoka, N.; Hayakawa, T. Beneficial Effects of the Genus *Aloe* on Wound Healing, Cell Proliferation, and Differentiation of Epidermal Keratinocytes. *PLoS One* **2016**, *11*, No. e0164799.
- (31) Mijit, M.; Caracciolo, V.; Melillo, A.; Amicarelli, F.; Giordano, A. Role of p53 in the Regulation of Cellular Senescence. *Biomolecules* **2020**, *10*, No. 420.
- (32) Berlanga-Acosta, J. A.; Guillén-Nieto, G. E.; Rodríguez-Rodríguez, N.; Mendoza-Mari, Y.; Bringas-Vega, M. L.; Berlanga-Saez, J. O.; García Del Barco, H. D.; Martínez-Jimenez, I.; Hernández-Gutiérrez, S.; Valdés-Sosa, P. A. Cellular Senescence as the Pathogenic Hub of Diabetes-Related Wound Chronicity. *Front. Endocrinol.* **2020**, *11*, No. 573032.
- (33) Ma, X. Y.; Cui, D.; Wang, Z.; Liu, B.; Yu, H. L.; Yuan, H.; Xiang, L. B.; Zhou, D. P. Silk Fibroin/Hydroxyapatite Coating Improved Osseointegration of Porous Titanium Implants under Diabetic Conditions via Activation of the PI3K/Akt Signaling Pathway. *ACS Biomater. Sci. Eng.* **2022**, *8*, 2908–2919.
- (34) Hu, Y.; Xu, J.; Hu, Q. Evaluation of Antioxidant Potential of *Aloe vera* (*Aloe barbadensis* Miller) Extracts. *J. Agric. Food Chem.* **2003**, *51*, 7788–7791.
- (35) Hoeben, A.; Landuyt, B.; Highley, M. S.; Wildiers, H.; Van-Oosterom, A. T.; De Bruijn, E. A. Vascular endothelial growth factor and angiogenesis. *Pharmacol. Rev.* **2004**, *56*, 549–580.
- (36) Firdaus, I.; Arfian, N.; Wahyuningsih, M. S. H.; Agustini, D. *Aloe vera* stimulate cell proliferation, cell migration, expression of vascular endothelial growth factor-A (VEGF-A), and c-Jun N-terminal kinase-1 (JNK-1) on fibroblast of diabetic rat models. *J. Med. Sci.* **2019**, *51*, 114–127.
- (37) Jettanacheawchankit, S.; Sasithanasate, S.; Sangvanich, P.; Banlunara, W.; Thunyakitpisal, P. Acemannan stimulates gingival fibroblast proliferation; expressions of keratinocyte growth factor-1, vascular endothelial growth factor, and type I collagen; and wound healing. *J. Pharmacol. Sci.* **2009**, *109*, 525–531.
- (38) Guo, Y. J.; Pan, W. W.; Liu, S. B.; Shen, Z. F.; Xu, Y.; Hu, L. L. ERK/MAPK signalling pathway and tumorigenesis. *Exp. Ther. Med.* **2020**, *19*, 1997–2007.
- (39) Avruch, J.; Khokhlatchev, A.; Kyriakis, J. M.; Luo, Z.; Tzivion, G.; Vavvas, D.; Zhang, X. F. Ras activation of the Raf kinase: tyrosine kinase recruitment of the MAP kinase cascade. *Recent Prog. Horm. Res.* **2001**, *56*, 127–155.
- (40) Di Paola, R.; Galuppo, M.; Mazzon, E.; Paterniti, I.; Bramanti, P.; Cuzzocrea, S. PD98059, a specific MAP kinase inhibitor, attenuates multiple organ dysfunction syndrome/failure (MODS) induced by zymosan in mice. *Pharmacol. Res.* **2010**, *61*, 175–187.
- (41) Maemura, K.; Shiraishi, N.; Sakagami, K.; Kawakami, K.; Inoue, T.; Murano, M.; Watanabe, M.; Otsuki, Y. Proliferative effects of gamma-aminobutyric acid on the gastric cancer cell line are associated with extracellular signal-regulated kinase 1/2 activation. *J. Gastroenterol. Hepatol.* **2009**, *24*, 688–696.
- (42) Liu, Y.; Fan, J.; Lv, M.; She, K.; Sun, J.; Lu, Q.; Han, C.; Ding, S.; Zhao, S.; Wang, G.; Zhang, Y.; Zang, G. Photocrosslinking silver nanoparticles-aloe vera-silk fibroin composite hydrogel for treatment of full-thickness cutaneous wounds. *Regen. Biomater.* **2021**, *8*, No. rbab048.
- (43) Ng, M. Y.; Lin, T.; Chao, S.-C.; Chu, P.-M.; Yu, C.-C. Potential Therapeutic Applications of Natural Compounds in Diabetes-Associated Periodontitis. *J. Clin. Med.* **2022**, *11*, No. 3614.